AD-A101 458 TENNESSEE UNIV KNOXVILLE DEPT OF CHEMISTRY F/G 7/4
EVALUATION OF LOW MELTING HALIDE SYSTEMS FOR BATTERY APPLICATIO--ETC(U)
MAR 81 G MAMANTOV, C PETROVIC F33615-78-C-2075
UNCLASSIFIED AFWAL-TR-81-2003 NL

1 OF 1
AD A
101458

END
DATE
FILMED
8-81
DTIC

AFWAL-TR-81-2003

EVALUATION OF LOW MELTING HALIDE SYSTEMS FOR BATTERY APPLICATIONS

Dr. G. Mamantov and Dr. C. Petrovic
University of Tennessee
Department of Chemistry
Knoxville, TN 37916

MARCH 1981

TECHNICAL REPORT AFWAL-TR-81-2003
Interim Report for Period September 1979 - September 1980

Approved for public release; distribution unlimited

AERO PROPULSION LABORATORY
AIR FORCE WRIGHT AERONAUTICAL LABORATORIES
AIR FORCE SYSTEMS COMMAND
WRIGHT-PATTERSON AIR FORCE BASE, OHIO 45433

NOTICE

When Government drawings, specifications, or other data are used for any purpose other than in connection with a definitely related Government procurement operation, the United States Government thereby incurs no responsibility nor any obligation whatsoever; and the fact that the government may have formulated, furnished, or in any way supplied the said drawings, specifications, or other data, is not to be regarded by implication or otherwise as in any manner licensing the holder or any other person or corporation, or conveying any rights or permission to manufacture use, or sell any patented invention that may in any way be related thereto.

This report has been reviewed by the Office of Public Affairs (ASD/PA) and is releasable to the National Technical Information Service (NTIS). At NTIS, it will be available to the general public, including foreign nations.

This technical report has been reviewed and is approved for publication.

James S. Cloyd

JAMES S. CLOYD
Project Engineer

Donald P. Mortel

DONALD P. MORTEL
TAM, Batteries & Fuel Cells
Energy Conversion Branch

FOR THE COMMANDER

J D Reams

JAMES D. REAMS
Chief, Aerospace Power Division
Aero Propulsion Laboratory

"If your address has changed, if you wish to be removed from our mailing list, or if the addressee is no longer employed by your organization please notify AFWAL/POOC-1 W-PAFB, OH 45433 to help us maintain a current mailing list".

Copies of this report should not be returned unless return is required by security considerations, contractual obligations, or notice on a specific document.

SECURITY CLASSIFICATION OF THIS PAGE (When Data Entered)

REPORT DOCUMENTATION PAGE

READ INSTRUCTIONS BEFORE COMPLETING FORM

1. REPORT NUMBER: AFWAL-TR-81-2003	2. GOVT ACCESSION NO.: AD-A101 458
3. RECIPIENT'S CATALOG NUMBER	
4. TITLE (and Subtitle): EVALUATION OF LOW MELTING HALIDE SYSTEMS FOR BATTERY APPLICATIONS	5. TYPE OF REPORT & PERIOD COVERED: Interim, 1 September 79 thru 30 September 80
	6. PERFORMING ORG. REPORT NUMBER
7. AUTHOR(s): Dr Gleb Mamantov, Dr Cedomir Petrovic	8. CONTRACT OR GRANT NUMBER(s): F33615-78-C-2075
9. PERFORMING ORGANIZATION NAME AND ADDRESS: University of Tennessee, Department of Chemistry, Knoxville TN 37919	10. PROGRAM ELEMENT, PROJECT, TASK AREA & WORK UNIT NUMBERS: 31452289
11. CONTROLLING OFFICE NAME AND ADDRESS: Air Force Wright Aeronautical Laboratories, Aero Propulsion Laboratory, Wright-Patterson AFB Ohio 45433	12. REPORT DATE: March 1981
	13. NUMBER OF PAGES: 64
14. MONITORING AGENCY NAME & ADDRESS (if different from Controlling Office)	15. SECURITY CLASS. (of this report): UNCLASSIFIED
	15a. DECLASSIFICATION/DOWNGRADING SCHEDULE

16. DISTRIBUTION STATEMENT (of this Report)

Approved for public release; distribution unlimited.

17. DISTRIBUTION STATEMENT (of the abstract entered in Block 20, if different from Report)

18. SUPPLEMENTARY NOTES

19. KEY WORDS (Continue on reverse side if necessary and identify by block number)

electrolytes, molten salt, low melting point, conductivity

20. ABSTRACT (Continue on reverse side if necessary and identify by block number)

This three year program involves evaluation of selected low temperature molten salt solvent systems containing inorganic and/or organic chlorides and bromides for battery applications. The research involves determination of the liquidus temperatures, the specific electrical conductivity, and the electrochemical span of selected halide systems. Characterization of the solvent species by Raman spectroscopy, vapor pressure measurements, and the electrochemical study of a few cathode and anode systems will be undertaken for the most promising solvent systems.

(Cont)

DD FORM 1 JAN 73 1473 EDITION OF 1 NOV 65 IS OBSOLETE

SECURITY CLASSIFICATION OF THIS PAGE (When Data Entered)

SECURITY CLASSIFICATION OF THIS P   When Data Entered)

The research during the second year of this project involved the determination of liquidus temperatures and/or specific electrical conductivities for a number of binary and ternary molten salt systems containing $AlCl_3$, $AlBr_3$, $SbCl_3$, $FeCl_3$, and $GaCl_3$.

SECURITY CLASSIFICATION OF THIS PAGE(When Data Entered)

FOREWORD

This report describes the work performed during the second year of a three-year program dealing with the experimental evaluation of some low melting halide systems for battery applications. This work was performed at the Department of Chemistry, The University of Tennessee, Knoxville, under Contract No. F33615-78-C-2075 with the Aero Propulsion Laboratory, Air Force Wright Aeronautical Laboratories, Wright-Patterson Air Force Base, Ohio. The principal investigator is Professor Gleb Mamantov. The Air Force Project officer is Mr. J. S. Cloyd, AFWAL/POOC, Wright-Patterson Air Force Base, Ohio.

The personnel working on the project consisted of Dr. Cedomir Petrovic, postdoctoral research associate, Jeff Cobb, Douglas Goff, and Robert Walton, undergraduate research assistants.

A

TABLE OF CONTENTS

LIST OF ILLUSTRATIONS

LIST OF TABLES

I. INTRODUCTION

The purpose of this three year project is to critically evaluate a wide range of binary and ternary low temperature molten salt systems for battery applications. These systems include chlorides and/or bromides of aluminum, antimony, iron and gallium as one component, and various alkali, alkaline earth, quaternary ammonium, n-butyl pyridinium and antimony chlorides and/or bromides as the other(s). Measurements of the liquidus range and the specific electrical conductivity are being performed on a number of the above systems. Vapor pressure, background voltammograms and Raman spectra will be studied for a few selected systems. Electrochemistry of selected cathode and anode materials will also be examined. The results of the first year of the work on this project have been presented in the Technical Report AFAPL-TR-79-2124 (1). This report covers the second year of the project.

During this period the liquidus range and/or electrical conductivity measurements have been performed on the following molten salt systems: $AlCl_3$-LiCl-NaCl, $AlCl_3$-NaBr, $AlBr_3$-NaCl, $AlBr_3$-Bu_4NBr, $AlBr_3$-Me_4NBr, $AlCl_3$-$SbCl_3$, $AlCl_3$-$SbCl_3$-n-BuPyCl, $FeCl_3$-NaCl, $FeCl_3$-LiCl-NaCl, and $GaCl_3$-NaCl.

Four molten salt systems have been selected for further work: $AlCl_3$-LiCl-NaCl, $AlCl_3$-$SbCl_3$-x (where x is a third chloride to be chosen), $FeCl_3$-LiCl-NaCl, and $AlCl_3$-Bu_4NCl. These salt systems will be studied in the third and last year of this project.

II. EXPERIMENTAL

The experimental aspects of the present work have been discussed in our Technical Report AFAPL-TR-79-2124 (1). The only changes in the equipment were the upgrading of the temperature stability of the furnace used for the electrical conductivity measurements by the addition of a Bayley Model 124 proportional temperature controller, and a recent change over from a chromel-alumel to a copper-constantan thermocouple, which has a superior reproducibility, for the temperature measurements.

Purified antimony chloride (Mallinckrodt, anhydrous, digested with antimony and distilled under vacuum) was obtained from the laboratory of Dr. G. P. Smith, Oak Ridge National Laboratory. Ferric chloride (Alfa-Ventron, anhydrous) was distilled under vacuum. Gallium chloride (Alfa-Ventron, 99.999%) was used as received.

III. $AlCl_3$-LiCl-NaCl SYSTEM

The $AlCl_3$-LiCl-NaCl system has been discussed in our Technical Report AFAPL-TR-79-2124 (1). Its low liquidus temperatures ($\geq$ 86°C), high specific conductivity (0.1 to 0.7 $ohm^{-1}cm^{-1}$ in the temperature range to 300°C); and a wide electrochemical span (>2.0V) make this molten salt system a very promising solvent for battery use. Our specific conductivity measurements on this system have been reported previously (1). Independent high precision conductivity measurements on the same system have been performed at the F. J. Seiler Research Laboratory (2).

Our phase diagram data for the two pseudobinary sections of the $AlCl_3$-LiCl-NaCl phase diagram (with the LiCl to NaCl mole ratios of 3:1 and 1:1) have also been reported (1). The new phase diagram data for the third pseudobinary section with the LiCl to NaCl mole ratio of 1:3 are listed in Table 1. This table also includes the additional data for the 3:1 and 1:1 sections. These data conclude our liquidus range measurements on the $AlCl_3$-LiCl-NaCl system. Figure 1 shows our combined data for the three pseudobinary sections of this system. The minimum in the liquidus curve of the 1:3 section is shifted by less than 2 mole % from the minimum in the 1:1 section. The solidus temperature in all three sections is the same (86°C). The only new feature of the data for the 1:3 section, which does not appear in the 1:1 section, is an intermediate phase transition at 97°C in the melts with less than 58 mole % $AlCl_3$, and at 103°C in the melts in which $AlCl_3$ is over 58 mole %. The nature of this transition is not clear.

IV. $AlCl_3$-NaBr SYSTEM

The addition of LiCl to the $AlCl_3$-NaCl system lowers its solidus temperature by 29°C without a significant change of the specific conductivity of this melt (1). In order to determine the effect of added bromide anion on the properties of the chloroaluminate melts we have studied the $AlCl_3$-NaBr system.

The phase diagram data for the $AlCl_3$-NaBr system have been presented previously (1). It was shown that the liquidus curve for the $AlCl_3$-NaBr system strongly resembles the liquidus curve for the $AlCl_3$-NaCl system, that the liquidus temperatures of the $AlCl_3$-NaBr system were lowered by as much as 32°C, and that the solidus temperatures (ranging from 72 to 86°) were a function of the mole fraction of the bromide ion.

Table 1

Phase Diagram Data for $AlCl_3$-LiCl-NaCl System

Composition (Mole %)			Solidus Temperature (°C)	Intermediate Transition (°C)	Liquidus Temperature (°C)
$AlCl_3$	LiCl	NaCl			
52.0	12.0	36.0	86	98*	128
54.0	11.5	34.5	86	?	120
56.0	11.0	33.0	86	96*	110
59.0	10.2	30.8	86	?	103#
60.0	10.0	30.0	86	103	113
62.0	9.5	28.5	86	103	130#
64.0	9.0	27.0	86	102	139
68.0	8.0	24.0	86	103	162
62.0	28.5	9.5	86		132
64.0	27.0	9.0	86		150
64.0	18.0	18.0	86		151

*Not reported previously

#Supercedes previously reported data

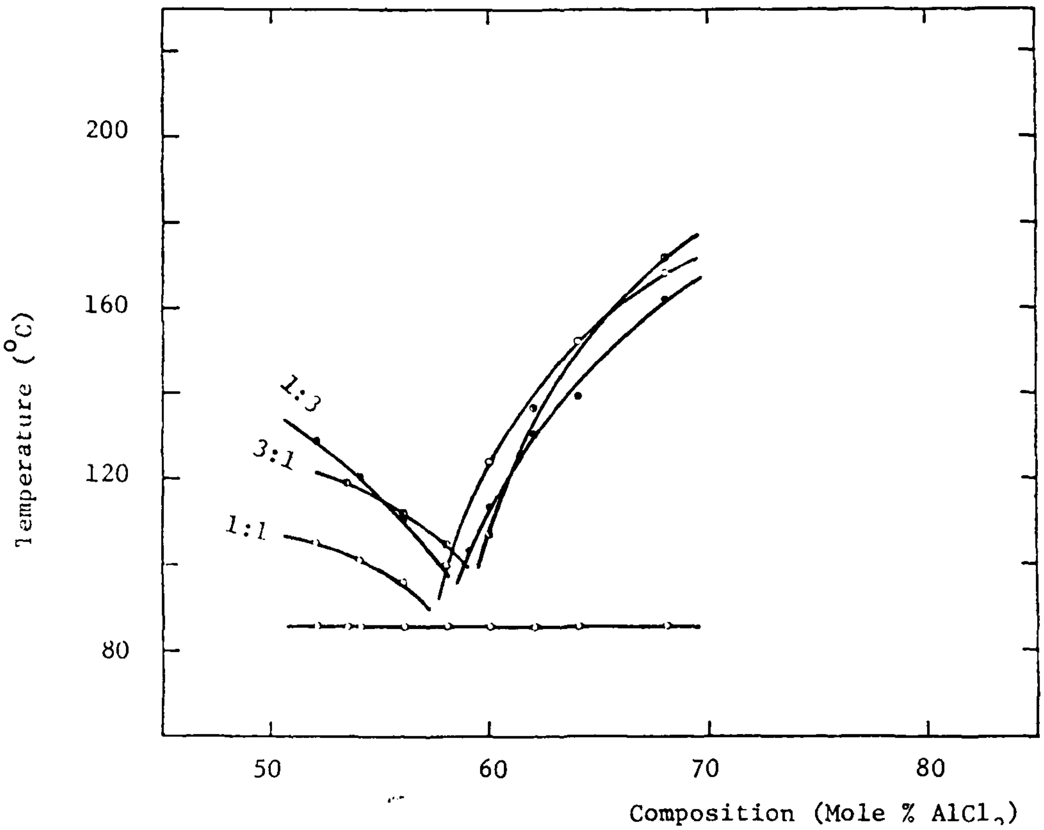

Figure 1. Phase Diagram Data for the $AlCl_3$-LiCl-NaCl System.
LiCl to NaCl mole ratios are indicated on the liquidus curves.

Our specific conductivity data for this system are listed in Tables 2 to 5, and shown in Figure 2. These conductivity vs. temperature plots are quite similar to the conductivity plots for the $AlCl_3$-LiCl-NaCl system which are also shown in the same figure. The difference in the specific conductivities of the two systems is within 7% for the 52.0 mole % $AlCl_3$ melts, and within 3% for the others. The specific conductivity of the pure bromide system, $AlBr_3$-NaBr, however, is lower than the conductivity of the $AlCl_3$-NaCl system by nearly an order of magnitude (3).

Based on the liquidus temperature and specific conductivity data, the system $AlCl_3$-NaBr is quite comparable to the $AlCl_3$-LiCl-NaCl system. However, literature data (4) indicate that the electrochemical span in the $AlCl_3$-NaBr system is 0.4 to 0.5V smaller than in the $AlCl_3$-NaCl system. From the battery use standpoint, this loss in the electrochemical span is not justified. About the same lowering of the liquidus temperatures of the $AlCl_3$-NaCl system can be accomplished by introducing LiCl as a third component, without paying any penalty in the electrochemical span.

V. $AlBr_3$-NaCl SYSTEM

Our phase diagram data for the $AlBr_3$-NaCl system, the second subsystem of the $AlCl_3$-$AlBr_3$-NaCl-NaBr system, are listed in Table 6 and shown in Figure 3. The similarity of our phase diagram data with the phase diagram of the corresponding pure bromide system $AlBr_3$-NaBr, which is also shown in Figure 3, is obvious. The lowering of the liquidus temperature of the pure bromide system by the addition of NaCl is only 7 to 10°C in the $AlBr_3$-rich composition region, and as much as 25°C in the region with less than 60 mole % $AlBr_3$. In that region, however, the liquidus temperatures of the $AlBr_3$-NaCl system are still above the liquidus temperatures of the $AlCl_3$-NaCl system. The bromide species, being in large excess, determines the shape of the phase diagram of this mixed chloride-bromide system. The measured liquidus temperatures in this system are as low as 94°C, but the eutectic temperature is outside the studied composition region ($\geq$ 72 mole % $AlBr_3$).

Our specific conductivity data for the $AlBr_3$-NaCl system are listed in Tables 7 to 10 and shown in Figure 4. The conductivity vs. temperature plots are nearly linear and qualitatively similar to the conductivity plots for the $AlCl_3$-LiCl-NaCl system, which are also shown in Figure 4. The values of the specific conductivity of the $AlBr_3$-NaCl melts, however, are

Table 2

Specific Conductivity Data for $AlCl_3$–NaBr System at 1.0 KHz

Composition: 52.0 - 48.0 (Mole %)

Temperature (^oC)	Specific Conductivity ($ohm^{-1} cm^{-1}$)
130.0	0.2386*
140.0	0.2654*
150.0	0.2919*
158.4	0.3147
169.3	0.3423
180.4	0.3703
190.8	0.3963
200.6	0.4207
210.1	0.4442
220.4	0.4698
229.4	0.4919
240.8	0.5186
250.9	0.5425
260.6	0.5660
269.4	0.5861
279.9	0.6095
290.2	0.6318
300.2	0.6530

* Calculated from Eqn. 1 (Ref. 1)

Table 3

Specific Conductivity Data for $AlCl_3$-NaBr System at 1.0 KHz

Composition: 60.0 - 40.0 (Mole %)

Temperature (^oC)	Specific Conductivity ($ohm^{-1} cm^{-1}$)
110.3	0.1275
120.2	0.1440
131.5	0.1634
141.0	o.1797
150.0	0.1955*
160.4	0.2134
171.4	0.2325
181.2	0.2499
190.0	0.2652
200.3	0.2834
210.2	0.3009
220.1	0.3183
230.4	0.3363
240.7	0.3544
250.3	0.3712

*Calculated from Eqn. 1 (Ref. 1)

Table 4

Specific Conductivity Data for $AlCl_3$-NaBr System at 1.0 KHz

Composition: 64.0 - 36.0 (Mole %)

Temperature (^oC)	Specific Conductivity ($ohm^{-1} cm^{-1}$)
120.0	o.1206*
130.4	0.1364
139.6	0.1498
150.9	0.1665
160.3	0.1808
170.0	0.1954
179.9	0.2104
189.9	0.2254
200.0	0.2410
209.6	0.2560
220.2	0.2722
230.0	0.2868
240.0	0.3024
249.8	0.3172

*Calculated from Eqn. 1

Table 5

Specific Conductivity Data for $AlCl_3$-NaBr System at 1.0 KHz

Composition: 68.0 - 32.0 (Mole %)

Temperature (°C)	Specific Conductivity ($ohm^{-1}cm^{-1}$)
169.7	0.1624
177.8	0.1727
188.8	0.1868
198.1	0.1988
208.5	0.2124
217.7	0.2250
229.4	0.2400
239.1	0.2532
250.6	0.2686

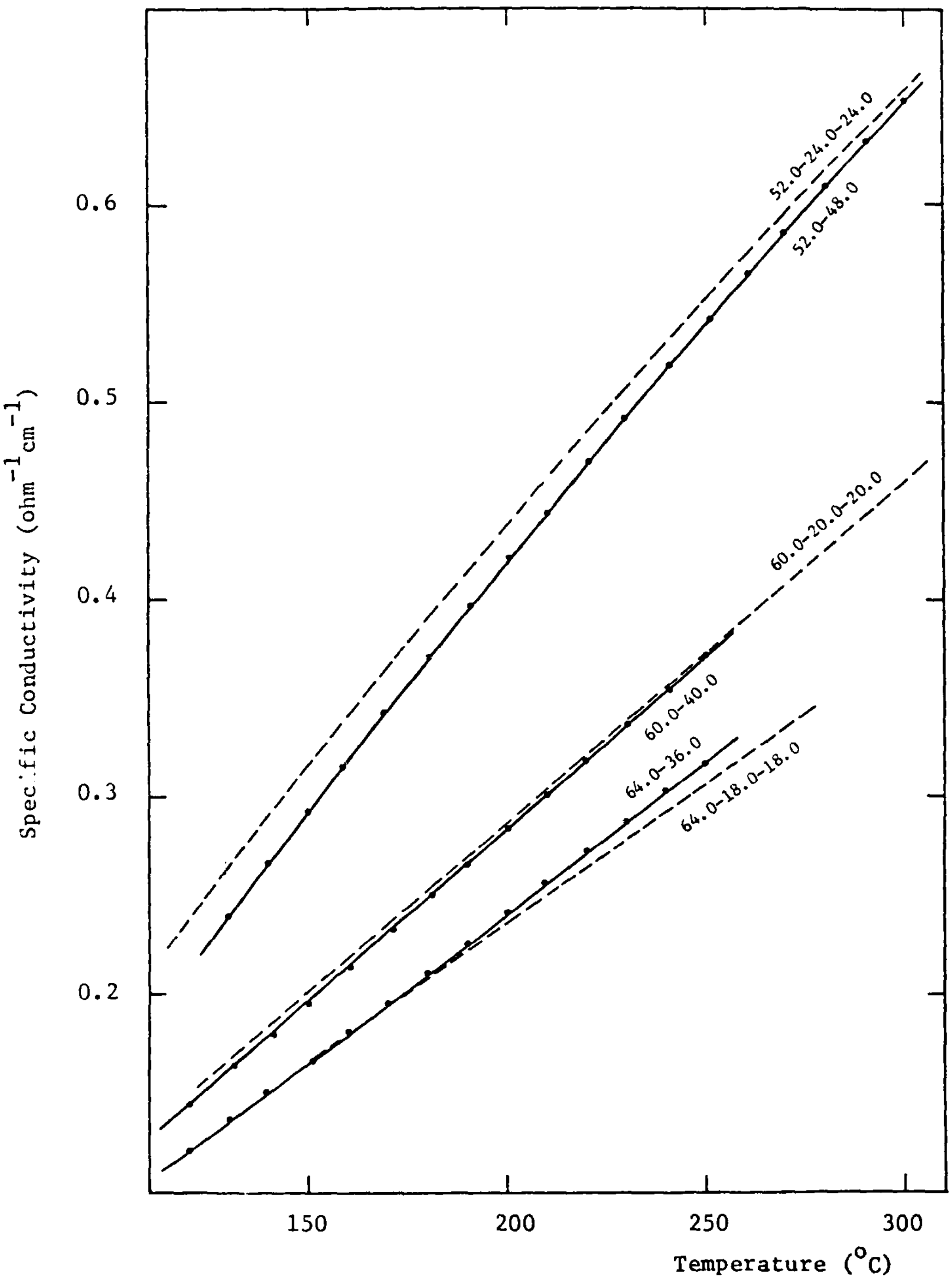

Figure 2. Specific Conductivity of $AlCl_3$-NaBr System (Full Line) and $AlCl_3$-LiCl-NaCl System (Dashed Line). Composition in mole % is indicated on the curves.

Table 6

Phase Diagram Data for $AlBr_3$-NaCl System

Composition (Mole %) $AlBr_3$	NaCl	Solidus Temperature (^oC)	Liquidus Temperature (^oC)
52.0	48.0	83	168
56.0	44.0	89	155
60.0	40.0	95	138
64.0	36.0	?	~114
68.0	32.0	81	97
72.0	28.0	82	94

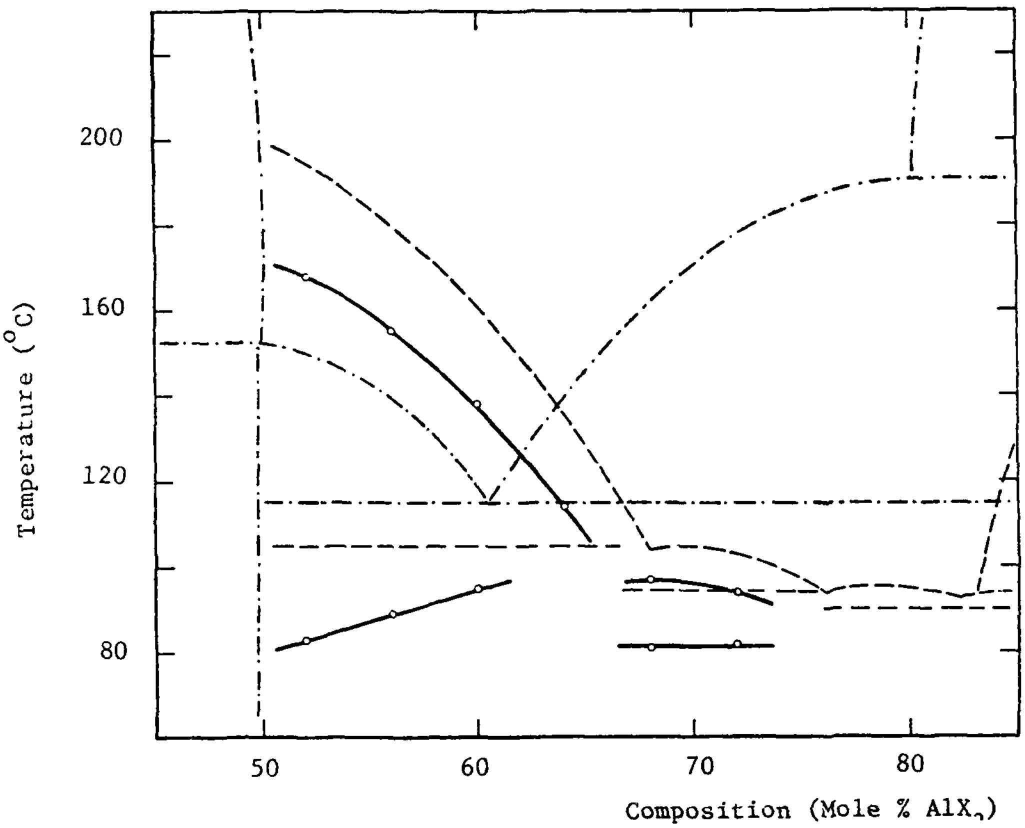

Figure 3. Phase Diagram Data for the $AlBr_3$-NaCl System. The phase diagrams of $AlBr_3$-NaBr system (dashed line) and $AlCl_3$-NaCl system (dot-dash line) are shown for reference.

Table 7

Specific Conductivity Data for $AlBr_3$-NaCl System at 1.0 KHz

Composition: 52.0 - 48.0 (Mole %)

Temperature (°C)	Specific Conductivity ($ohm^{-1}cm^{-1}$)
188.6	0.3189
198.4	0.3408
209.4	0.3637
218.9	0.3848
228.9	0.4065
238.9	0.4281
249.5	0.4507
259.6	0.4718
270.7	0.4947
280.2	0.5141
290.6	0.5346
299.5	0.5521

Table 8

Specific Conductivity Data for $AlBr_3$-NaCl System at 1.0 KHz

Composition: 56.0 - 44.0 (Mole %)

Temperature (°C)	Specific Conductivity ($ohm^{-1} cm^{-1}$)
177.6	0.2318
189.2	0.2532
199.8	0.2729
208.5	0.2887
219.0	0.3079
229.8	0.3277
239.6	0.3456
249.6	0.3634

Table 9

Specific Conductivity Data for $AlBr_3$-NaCl System at 1.0 KHz

Composition: 64.0 - 36.0 (Mole %)

Temperature (°C)	Specific Conductivity ($ohm^{-1} cm^{-1}$)
137.7	0.09986
147.4	0.1115
158.8	0.1256
169.5	0.1389
178.9	0.1508
188.2	0.1626
198.7	0.1760
208.2	0.1882
219.7	0.2029
229.3	0.2157
238.7	0.2278
249.7	0.2421

Table 10

Specific Conductivity Data for $AlBr_3$-NaCl System at 1.0 KHz

Composition: 68.0 - 32.0 (Mole %)

Temperature (°C)	Specific Conductivity ($ohm^{-1}cm^{-1}$)
119.1	0.06191
130.9	0.07299
138.8	0.08052
149.5	0.09121
159.6	0.1014
171.0	0.1132
180.9	0.1234
189.7	0.1325
199.6	0.1428
209.9	0.1535
220.8	0.1653
229.8	0.1748
240.4	0.1862
250.3	0.1971

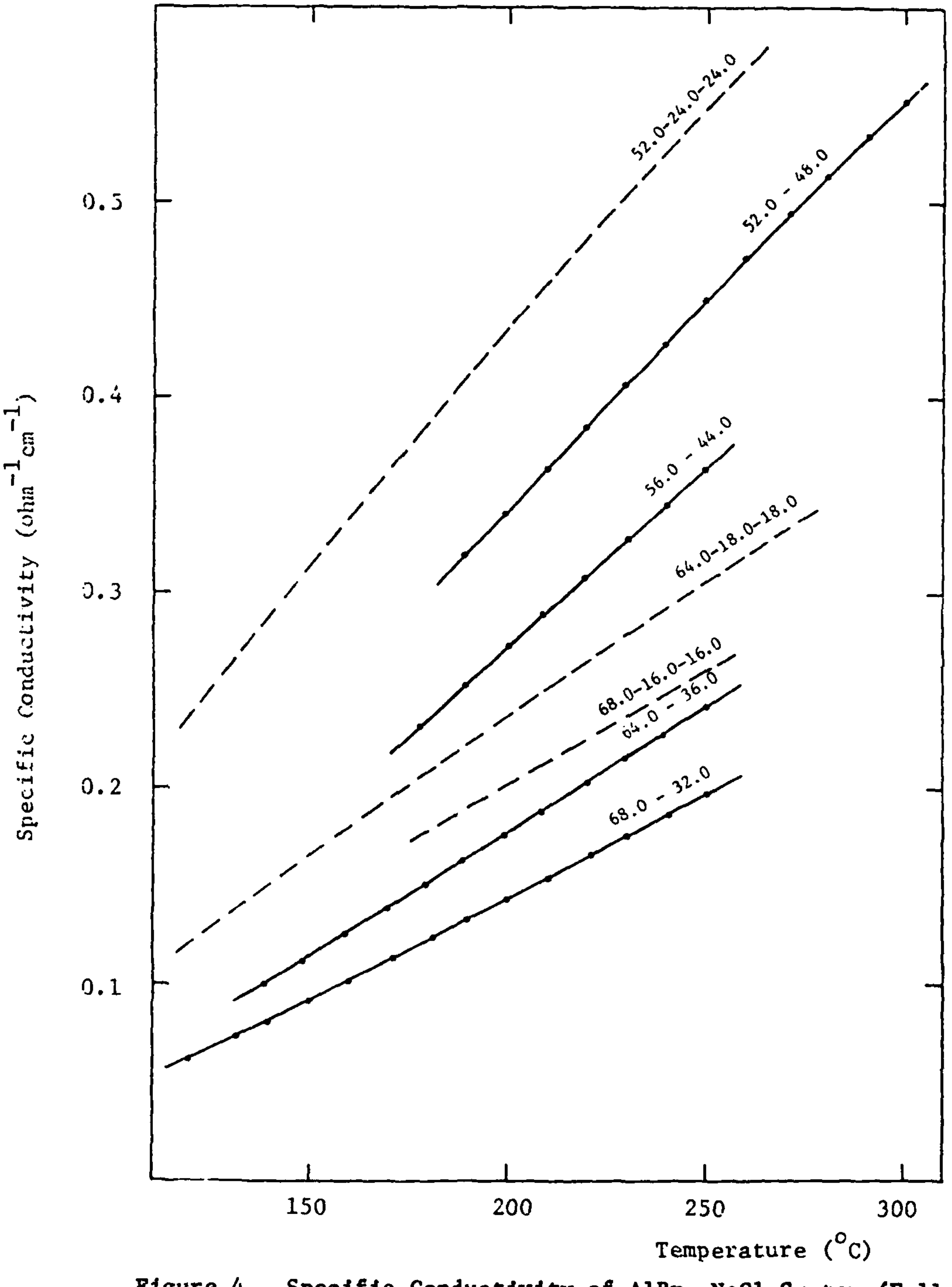

Figure 4. Specific Conductivity of $AlBr_3$-NaCl System (Full Line) and $AlCl_3$-LiCl-NaCl System (Dashed Line). Composition in mole % is indicated on the curves.

considerably lower ($\sim$ 20% for the 52.0-48.0 mole % melt, and up to 30% at 68.0 mole % $AlBr_3$).

In summary, the low melting region of the $AlBr_3$-NaCl system is shifted towards highly acidic compositions, so that the liquidus temperatures below 62 mole % $AlBr_3$ are actually higher than in the $AlCl_3$-NaCl system. The specific conductivity of the $AlBr_3$-NaCl system is 20 to 30% lower than in the $AlCl_3$-LiCl-NaCl system. Based on these data, the $AlBr_3$-NaCl system does not seem to offer much promise for the battery use.

VI. $AlBr_3$-Bu_4NBr SYSTEM

The $AlBr_3$-Bu_4NBr system has been discussed previously (1). Based on the low melting point of the pure Bu_4NBr ($\geq$ 101°C) (5), the $AlBr_3$-Bu_4NBr system was expected to be a very low melting system. Our preliminary experiments indicated that the liquidus temperatures of the melts with more than 50 mole % Bu_4NBr were indeed below room temperature (1). Subsequent experiments have shown, however, that these melts were merely supercooled for unusually long periods of time ($\sim$ 9 months for the 40.0-60.0 mole % melt, and $\sim$ 1 year for the 30.0-70.0 mole % melt). The true liquidus temperature of these two melts, determined by the visual method, was 111°C for the 40.0-60.0 mole % melt, and 89°C for the 30.0-70.0 mole % melt. The solidus temperature in the Bu_4NBr-rich composition region is 62°C. Therefore, our statement in Technical Report AFAPL-TR-79-2124 (1) about the room temperature melts of the $AlBr_3$-Bu_4NBr system is being withdrawn.

Our specific conductivity data for the $AlBr_3$-Bu_4NBr system are listed in Tables 11 to 16 and shown in Figure 5. The conductivity of these melts, less than 0.03 $ohm^{-1}cm^{-1}$ at 220°C, is quite low. In view of the high viscosity of these melts, however, and of the large size of the Bu_4N^+ cation, which is presumably the conducting species in these melts, such low specific conductivity seems to be reasonable. The conductivity vs. temperature plots exhibit a very pronounced curvature. The conductivity at a given temperature has little dependence on the composition of the melt, with the exception of the 30.0-70.0 mole % melt. This may be a result of the increase in the molar volume with the increasing mole fraction of Bu_4NBr.

In summary, even though the liquidus temperatures in the $AlBr_3$-Bu_4NBr melts are quite low ($\geq$ 62°C), their very low specific conductivity, as well as their electrochemical span, smaller by 0.4 to 0.5V than in the chloride

Table 11

Specific Conductivity Data for $AlBr_3$-Bu_4NBr System at 1.0 KHz

Composition 30.0 - 70.0 (Mole %)

Temperature (°C)	Specific Conductivity ($ohm^{-1}cm^{-1}$)
95.4	0.001238
105.1	0.001736
114.3	0.002328
125.2	0.003190
135.5	0.004159
144.8	0.005252
154.2	0.006587
164.8	0.008356
172.8	0.010221
182.9	0.012342
195.0	0.015118
205.3	0.017712
214.9	0.020414

Table 12

Specific Conductivity Data for $AlBr_3$-Bu_4NBr System at 1.0 KHz

Composition 40.0 - 60.0 (Mole %)

Temperature (°C)	Specific Conductivity ($ohm^{-1}cm^{-1}$)
127.1	0.006026
137.9	0.007592
147.2	0.009165
157.6	0.011114
167.6	0.013130
176.5	0.015143
186.8	0.017667
196.0	0.020560

Table 13

Specific Conductivity Data for $AlBr_3$-Bu_4NBr System at 1.0 KHz

Composition: 50.0 - 50.0 (Mole %)

Temperature (°C)	Specific Conductivity ($ohm^{-1} cm^{-1}$)
152.1	0.01049
161.2	0.01235
171.2	0.01448
180.4	0.01669
189.2	0.01883
198.6	0.02136
209.1	0.02427
218.6	0.02696

Table 14

Specific Conductivity Data for $AlBr_3$-Bu_4NBr System at 1.0 KHz

Composition: 60.0 - 40.0 (Mole %)

Temperature (°C)	Specific Conductivity ($ohm^{-1} cm^{-1}$)
113.9	0.004614
118.6	0.005142
122.7	0.005609
128.4	0.006297
135.2	0.007195
145.2	0.008585
154.2	0.009871
163.3	0.01152
172.4	0.01312

Table 15

Specific Conductivity Data for $AlBr_3$-Bu_4NBr System at 1.0 KHz

Composition: 64.0 - 36.0 (Mole %)

Temperature (°C)	Specific Conductivity ($ohm^{-1} cm^{-1}$)
99.2	0.003440
110.5	0.004499
118.6	0.005361
129.3	0.006654
139.4	0.007970
150.0	0.009484
160.4	0.01112
171.1	0.01291
181.6	0.01478
193.5	0.01704
200.6	0.01843
209.4	0.02022
219.0	0.02223

Table 16

Specific Conductivity Data for $AlBr_3$-Bu_4NBr System at 1.0 KHz

Composition: 68.0 - 32.0 (Mole %)

Temperature (°C)	Specific Conductivity ($ohm^{-1} cm^{-1}$)
85.0	0.002423
92.5	0.002966
102.2	0.003758
112.3	0.004685
122.5	0.005743
133.8	0.007053
144.8	0.008438
157.7	0.01024
169.5	0.01206
178.5	0.01351
192.2	0.01585
203.9	0.01796
212.6	0.01958
219.6	0.02092

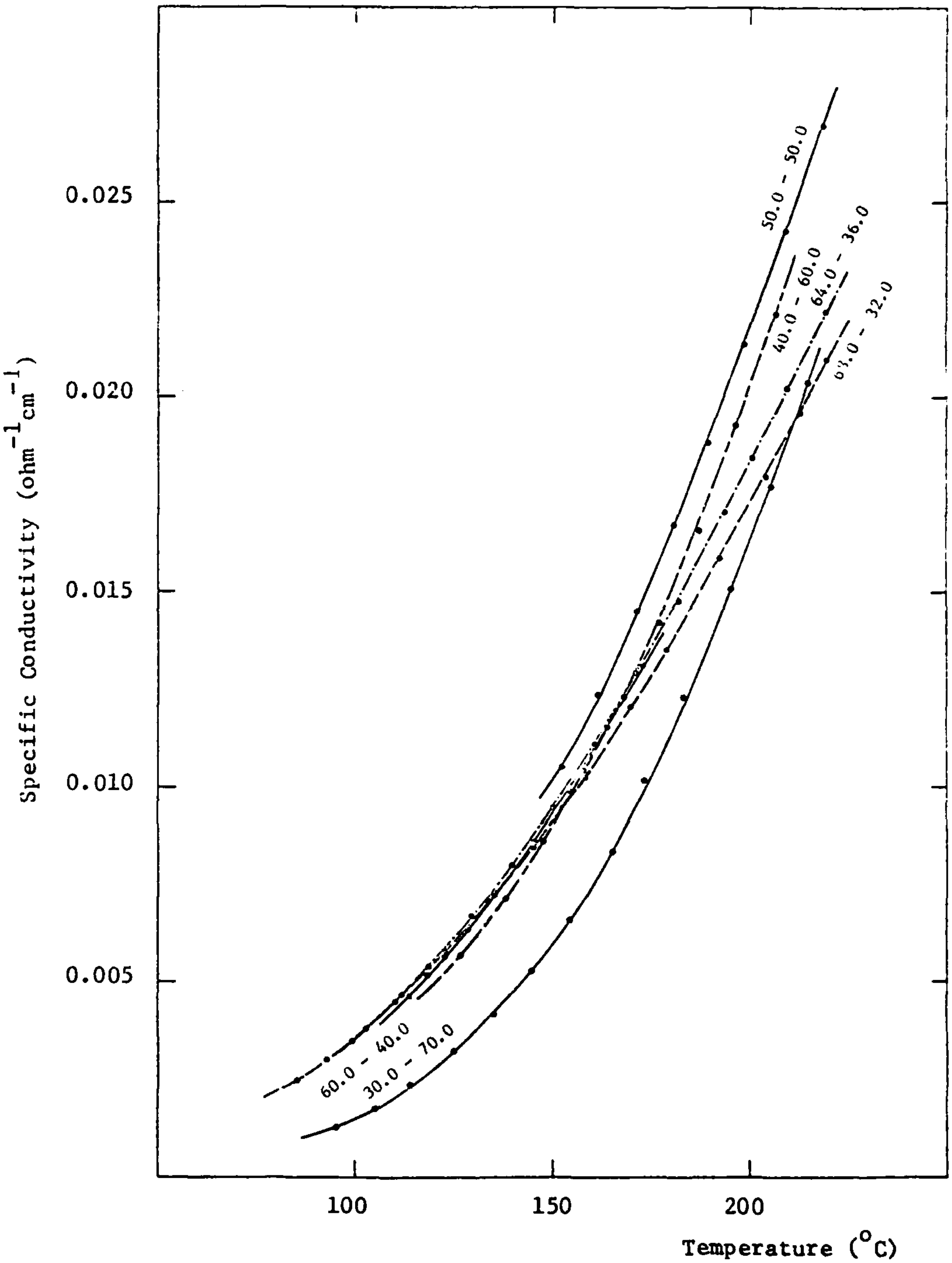

Figure 5. Specific Conductivity of $AlBr_3$-Bu_4NBr System. Composition in mole % is indicated on the curves.

melts, severely limit the potential usefulness of these melts for battery applications.

VII. $AlBr_3$-Me_4NBr SYSTEM

The $AlBr_3$-Me_4NBr system has also been discussed previously (1). The pure Me_4NBr decomposes without melting at ∿ 230°C (6), and its mixtures with less than 50 mole % $AlBr_3$ decompose before reaching the liquidus temperature. The solidus temperature in the $AlBr_3$-rich composition region is in the 70–80°C range. Our specific conductivity data for the 70.0-30.0 mole % $AlBr_3$-Me_4NBr melt are listed in Table 17 and shown in Figure 6. These conductivity data are ∿ 70% higher than the values for the 68.0-32.0 mole % $AlBr_3$-Bu_4NBr melt at the same temperature. This higher conductivity is presumably due to the smaller size and consequently higher mobility of the Me_4N^+ cation compared to the Bu_4N^+ cation. The conductivity of the $AlCl_3$-Me_4NBr melt, however, is still too low to justify a further study of this system.

VIII. $AlCl_3$-$SbCl_3$ SYSTEM

The phase diagram of the $AlCl_3$-$SbCl_3$ system, based on the data of Kendall et al., (7) and Niselson et al., (8) is shown in Figure 7. The eutectic temperature in this system is 70°C, and the eutectic composition is ∿ 10 mole % $AlCl_3$. Since $SbCl_3$ is a weaker acid than $AlCl_3$, an acid-base equilibrium is expected to take place in their binary melts:

$$2SbCl_3+Al_2Cl_6 \rightleftarrows 2SbCl_2^+ +2AlCl_4^-.$$

However, the phase diagram of this system (Figure 7), gives no indication of the formation of a compound in the solid phase. Moreover, the Raman studies show no evidence for the presence of the $AlCl_4^-$ or $Al_2Cl_7^-$ ions in these melts (9). Since the molten pure $AlCl_3$ and $SbCl_3$ are both nonconducting molecular liquids, the electrical conductivity of the $AlCl_3$-$SbCl_3$ melts is expected to be very low.

Our specific conductivity data for the $AlCl_3$-$SbCl_3$ system are listed in Tables 18 to 28, and shown in Figures 8 and 9. The observed relatively high specific conductivity of the order of 0.05 to 0.09 $ohm^{-1}cm^{-1}$, (∿ 20% of the conductivity of the $AlCl_3$-LiCl-NaCl melts) is quite surprising. The conductivity vs. temperature plots exhibit a pronounced curvature, particularly at

Table 17

Specific Conductivity Data for $AlBr_3$-Me_4NBr System at 1.0 KHz

Composition: 70.0 - 30.0 (Mole %)

Temperature (°C)	Specific Conductivity ($ohm^{-1}cm^{-1}$)
108.4	0.00728
118.3	0.00887
129.8	0.0110
144.8	0.0141
148.4	0.0150
167.3	0.0196
188.2	0.0254
208.0	0.0314
224.2	0.0367

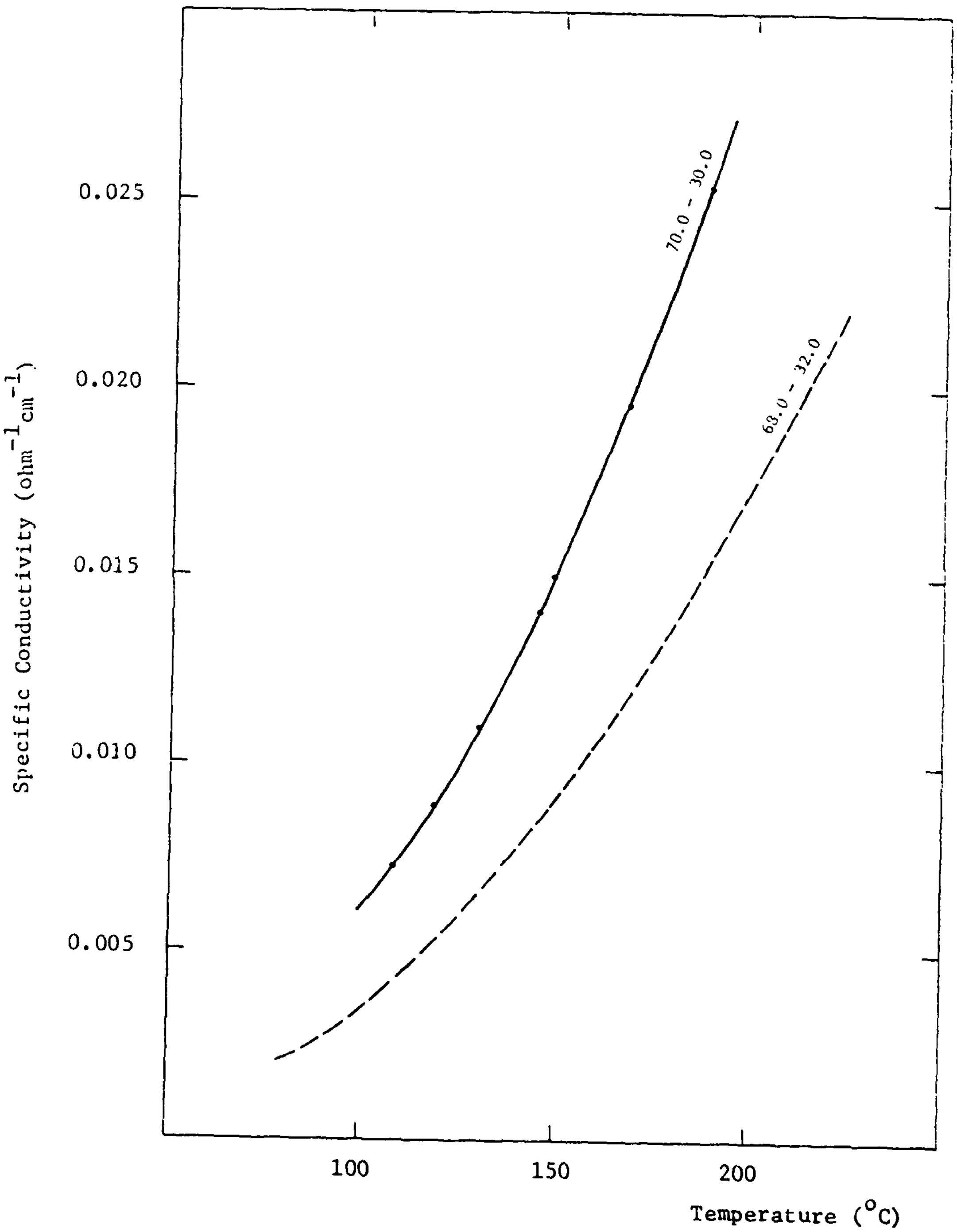

Figure 6. Specific Conductivity of $AlBr_3$-Me_4NBr 70.0-30.0 Mole % Melt (Full Line) and $AlBr_3$-Bu_4NBr 68.0-32.0 Mole % Melt (Dashed Line).
Composition in mole % is indicated on the curves.

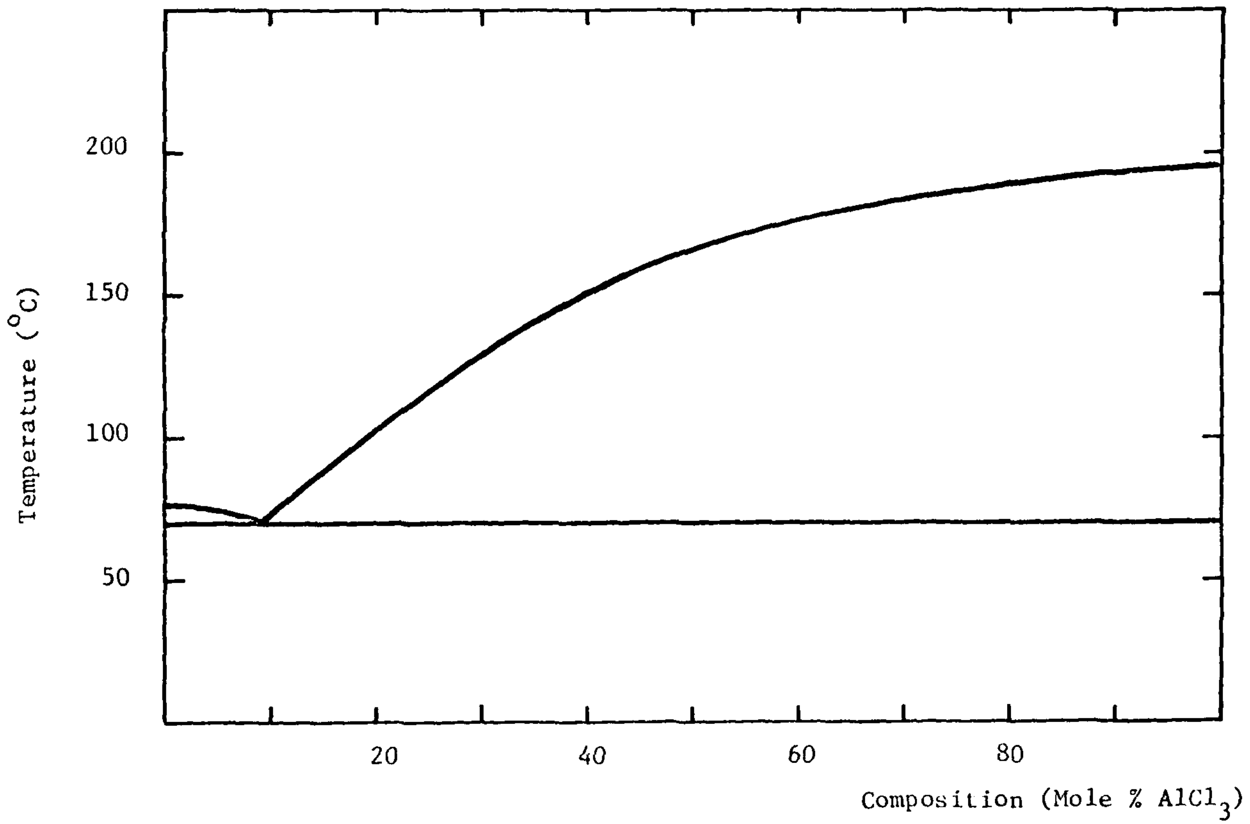

Figure 7. Phase Diagram of the $AlCl_3$-$SbCl_3$ System.

Table 18

Specific Conductivity Data for $AlCl_3$-$SbCl_3$ System at 1.0 KHz.

Composition: 2.5 - 97.5 (Mole %)

Temperature (°C)	Specific Conductivity ($ohm^{-1}cm^{-1}$)
86.7	0.007845
95.6	0.008355
106.6	0.008919
116.6	0.009367
126.8	0.009750
134.9	0.010010
144.3	0.010255
154.6	0.010469
167.8	0.010638
178.0	0.010699
187.0	0.010708
200.2	0.010652
204.4	0.010601
212.9	0.010511
222.5	0.010364
231.3	0.010197

Table 19

Specific Conductivity Data for $AlCl_3$-$SbCl_3$ System at 1.0 KHz

Composition: 5.0 - 95.0 (Mole %)

Temperature (°C)	Specific Conductivity ($ohm^{-1}cm^{-1}$)
83.8	0.01399
93.1	0.01514
102.8	0.01623
113.2	0.01735
123.3	0.01825
134.0	0.01908
144.2	0.01974
154.1	0.02027
164.0	0.02071
173.8	0.02101
185.4	0.02122
193.3	0.02129
201.2	0.02133
206.5	0.02126
211.6	0.02120
217.6	0.02110
226.0	0.02089
232.0	0.02070

Table 20

Specific Conductivity Data for $AlCl_3$-$SbCl_3$ System at 1.0 KHz

Composition: 10.0 - 90.0 (Mole %)

Temperature (°C)	Specific Conductivity ($ohm^{-1} cm^{-1}$)
80.2	0.02326
90.0	0.02610
101.2	0.02864
109.9	0.03070
119.4	0.03276
129.2	0.03473
138.9	0.03646
148.7	0.03802
158.3	0.03938
167.6	0.04048
170.8	0.04090
180.1	0.04176
190.8	0.04252
199.8	0.04294
208.7	0.04320
218.9	0.04331
229.6	0.04320

Table 21

Specific Conductivity Data for $AlCl_3$-$SbCl_3$ System at 1.0 KHz

Composition: 15.0 - 85.0 (Mole %)

Temperature (°C)	Specific Conductivity ($ohm^{-1}cm^{-1}$)
108.8	0.03951
119.2	0.04306
128.8	0.04613
138.3	0.04891
147.8	0.05152
150.1	0.05214
157.0	0.05385
158.5	0.05415
170.2	0.05673
178.8	0.05837
190.0	0.06018
191.8	0.06051
200.0	0.06150
201.4	0.06171
210.8	0.06262
221.1	0.06329
230.2	0.06363
239.8	0.06370

Table 22

Specific Conductivity Data for $AlCl_3$-$SbCl_3$ System at 1.0 KHz

Composition: 20.0 - 80.0 (Mole %)

Temperature (°C)	Specific Conductivity ($ohm^{-1} cm^{-1}$)
123.0	0.05071
128.0	0.05285
132.2	0.05447
132.7	0.05480
140.5	0.05787
144.4	0.05942
150.8	0.06171
158.0	0.06430
162.0	0.06563
169.3	0.06801
172.1	0.06886
183.6	0.07223
197.4	0.07551
209.0	0.07771
217.3	0.07897
226.0	0.07998

Table 23

Specific Conductivity Data for $AlCl_3$-$SbCl_3$ System at 1.0 KHz

Composition: 25.0 - 75.0 (Mole %)

Temperature (°C)	Specific Conductivity ($ohm^{-1} cm^{-1}$)
125.5	0.05378
128.4	0.05527
137.5	0.05961
148.2	0.06461
160.4	0.07001
170.2	0.07407
182.4	0.07869
193.6	0.08242
204.6	0.08561
215.0	0.08815
225.1	0.09016

Table 24

Specific Conductivity Data for $AlCl_3$-$SbCl_3$ System at 1.0 KHz

Composition: 30.0 - 70.0 (Mole %)

Temperature (°C)	Specific Conductivity (ohm^{-1} cm^{-1})
160.8	0.07205
168.2	0.07566
171.7	0.07728
172.4	0.07767
179.0	0.08067
184.8	0.08320
191.1	0.08579
197.1	0.08811
203.9	0.09058
209.2	0.09243
213.6	0.09382
217.0	0.09484
220.2	0.09575

Table 25

Specific Conductivity Data for $AlCl_3$-$SbCl_3$ System at 1.0 KHz

Composition: 40.0 - 60.0 (Mole %)

Temperature (°C)	Specific Conductivity ($ohm^{-1} cm^{-1}$)
173.6	0.07461
177.3	0.07661
179.3	0.07835
185.5	0.08083
191.1	0.08400
197.4	0.08674
201.4	0.08891
204.9	0.09037
211.4	0.09311
214.0	0.09428
217.8	0.09575

Table 26

Specific Conductivity Data for $AlCl_3$-$SbCl_3$ System at 1.0 KHz

Composition: 50.0 - 50.0 (Mole %)

Temperature (°C)	Specific Conductivity ($ohm^{-1} cm^{-1}$)
181.7	0.06879
191.9	0.07444
192.2	0.07455
197.2	0.07704
201.2	0.07904
202.0	0.07933
210.3	0.08282

Table 27

Specific Conductivity Data for $AlCl_3$-$SbCl_3$ System at 1.0 KHz

Composition: 55.0 - 45.0 (Mole %)

Temperature (°C)	Specific Conductivity ($ohm^{-1}cm^{-1}$)
183.1	0.06313
186.3	0.06486
189.4	0.06637
194.4	0.06854
198.3	0.07012
200.6	0.07156
203.4	0.07242
205.2	0.07351
208.4	0.07470
212.8	0.07666
218.0	0.07880

Table 28

Specific Conductivity Data for $AlCl_3$-$SbCl_3$ System at 1.0 KHz

Composition: 60.0 - 40.0 (Mole %)

Temperature (°C)	Specific Conductivity ($ohm^{-1}cm^{-1}$)
193.3	0.06271
195.0	0.06344
202.0	0.06620
206.6	0.06747
211.6	0.06941
216.7	0.07125

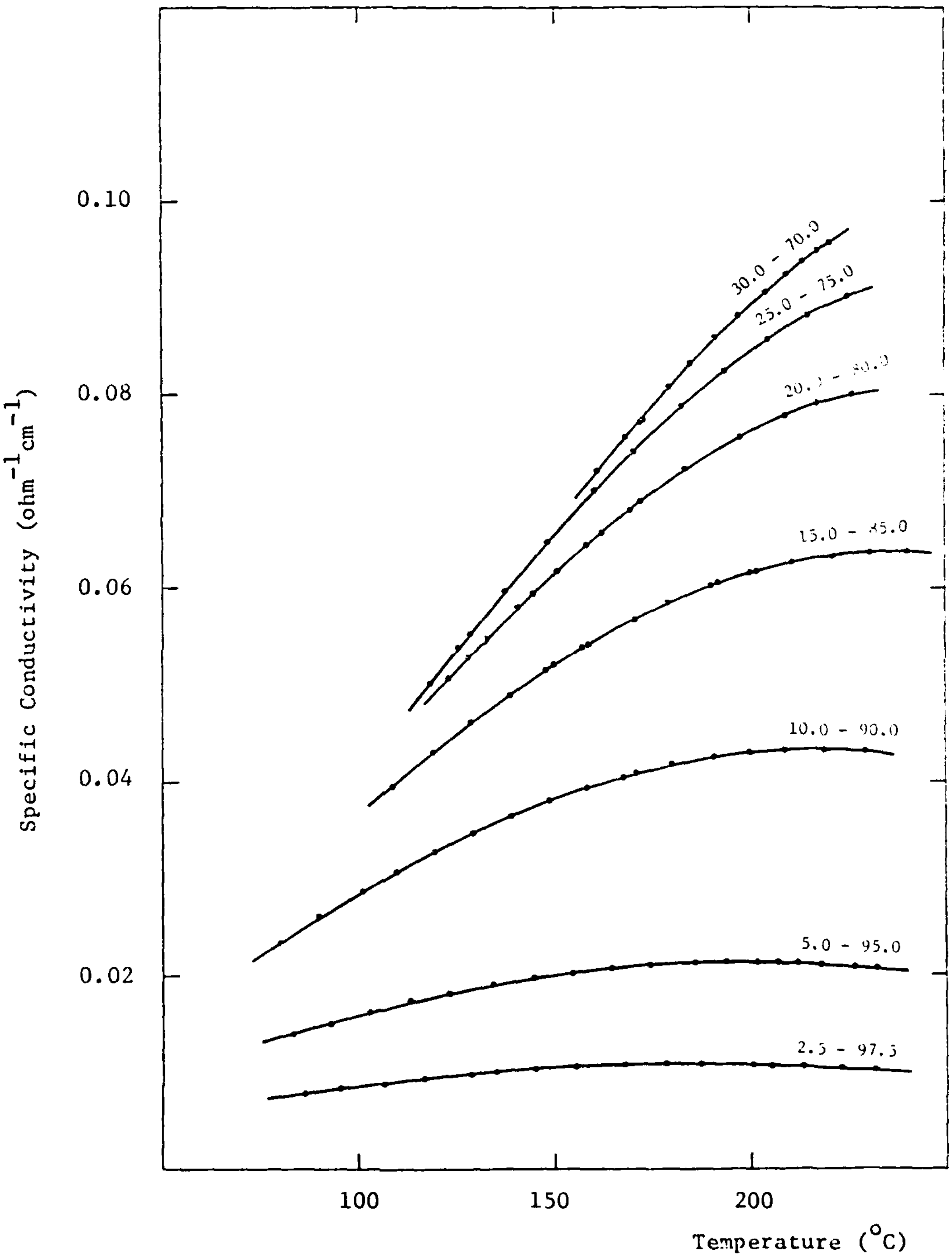

Figure 8. Specific Conductivity of $AlCl_3$-$SbCl_3$ System (Part 1). Composition in mole % is indicated on the curves.

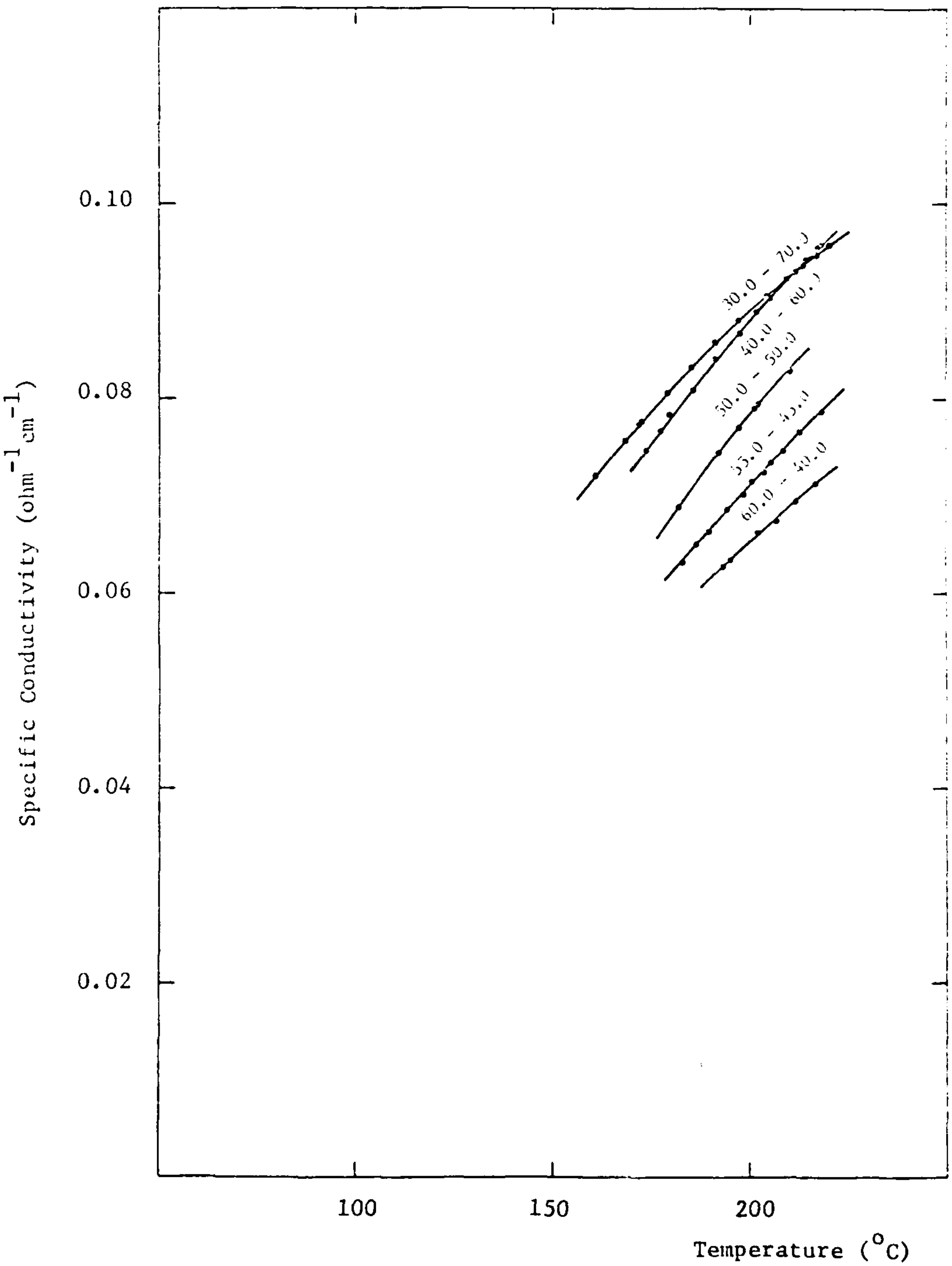

Figure 9. Specific Conductivity of $AlCl_3$-$SbCl_3$ System (Part 2). Composition in mole % is indicated on the curves.

low mole fractions of $AlCl_3$. The plots for the melts with 10 mole % $AlCl_3$ or less exhibit a maximum. The specific conductivity at constant temperature reaches a maximum at a composition between 30 and 35 mole % $AlCl_3$. A detailed evaluation of the experimental results obtained on this system is currently in progress.

Our conductivity measurements on the 60.0-40.0 mole % melt are not very reproducible. This appears to be due to the high volatility of this melt even at temperatures close to its liquidus point. Therefore, no conductivity measurements were performed on the melts with more than 60 mole % $AlCl_3$.

In summary, the $AlCl_3$-$SbCl_3$ melts have very low liquidus temperatures, and unexpectedly high specific conductivity. The melts with less than 50 mole % $AlCl_3$ seem to be promising for use in batteries in which $SbCl_3$ is used as a cathode material.

IX. $AlCl_3$-$SbCl_3$-n-BuPyCl SYSTEM

Samples of the $AlCl_3$-$SbCl_3$-n-BuPyCl melts were obtained from the laboratory of Dr. G. P. Smith at Oak Ridge National Laboratory. Since the liquidus temperature of the two compositions studied, 19.0-60.0-21.0 and 21.0-60.0-19.0 mole %, is below 25% C, we have performed no phase diagram measurements. The results of our specific conductivity measurements are listed in Tables 29 and 30, and shown in Figure 10. The conductivity data for the 25.0-75.0 mole % $AlCl_3$-$SbCl_3$, which has approximately the same $AlCl_3$ to $SbCl_3$ mole ratio as the two ternary n-BuPyCl melts, are shown for comparison in the same figure.

The addition of n-BuPyCl to the $AlCl_3$-$SbCl_3$ melt has a very pronounced effect on its specific conductivity. In the low temperature region, below $\sim$ 100°C, the conductivity vs. temperature plots become increasingly nonlinear. Also, the specific conductivity of the $AlCl_3$-$SbCl_3$-n-BuPyCl ternary melts is $\sim$ 40% lower than the conductivity of the corresponding 25.0-75.0 mole % $AlCl_3$-$SbCl_3$ binary melt at the same temperature. The factors responsible for this significant decrease in conductivity are currently under study at Oak Ridge National Laboratory.

From the practical point of view, however, the lowering of the liquidus temperatures in the $AlCl_3$-$SbCl_3$-n-BuPyCl melts is offset by the large decrease in the specific conductivity of the $AlCl_3$-$SbCl_3$ melts. Therefore, no more additional work is planned on the $AlCl_3$-$SbCl_3$-n-BuPyCl system during the coming year.

Table 29

Specific Conductivity Data for $AlCl_3$-$SbCl_3$-n-BuPyCl System
at 1.0 KHz

Composition: 19.0 - 60.0 - 21.0 (Mole %)

Temperature (°C)	Specific Conductivity ($ohm^{-1} cm^{-1}$)
24.4	0.003947
36.5	0.006524
44.3	0.008438
49.2	0.009756
59.3	0.01275
68.2	0.01570
79.1	0.01954
89.7	0.02357
99.8	0.02759
107.8	0.03087
119.8	0.03595
129.8	0.04024
139.9	0.04470
149.9	0.04922
160.8	0.05422

Table 30

Specific Conductivity Data for $AlCl_3$-$SbCl_3$-n-BuPyCl System at 1.0 KHz

Composition: 21.0 - 60.0 - 19.0 (Mole %)

Temperature (°C)	Specific Conductivity ($ohm^{-1} cm^{-1}$)
24.4	0.003979
36.8	0.006289
44.2	0.007912
49.3	0.009099
59.3	0.01163
68.2	0.01413
79.0	0.01732
89.7	0.02071
99.8	0.02408
107.4	0.02665
119.9	0.03103
129.7	0.03455
139.9	0.03828
149.8	0.04203
160.8	0.04624

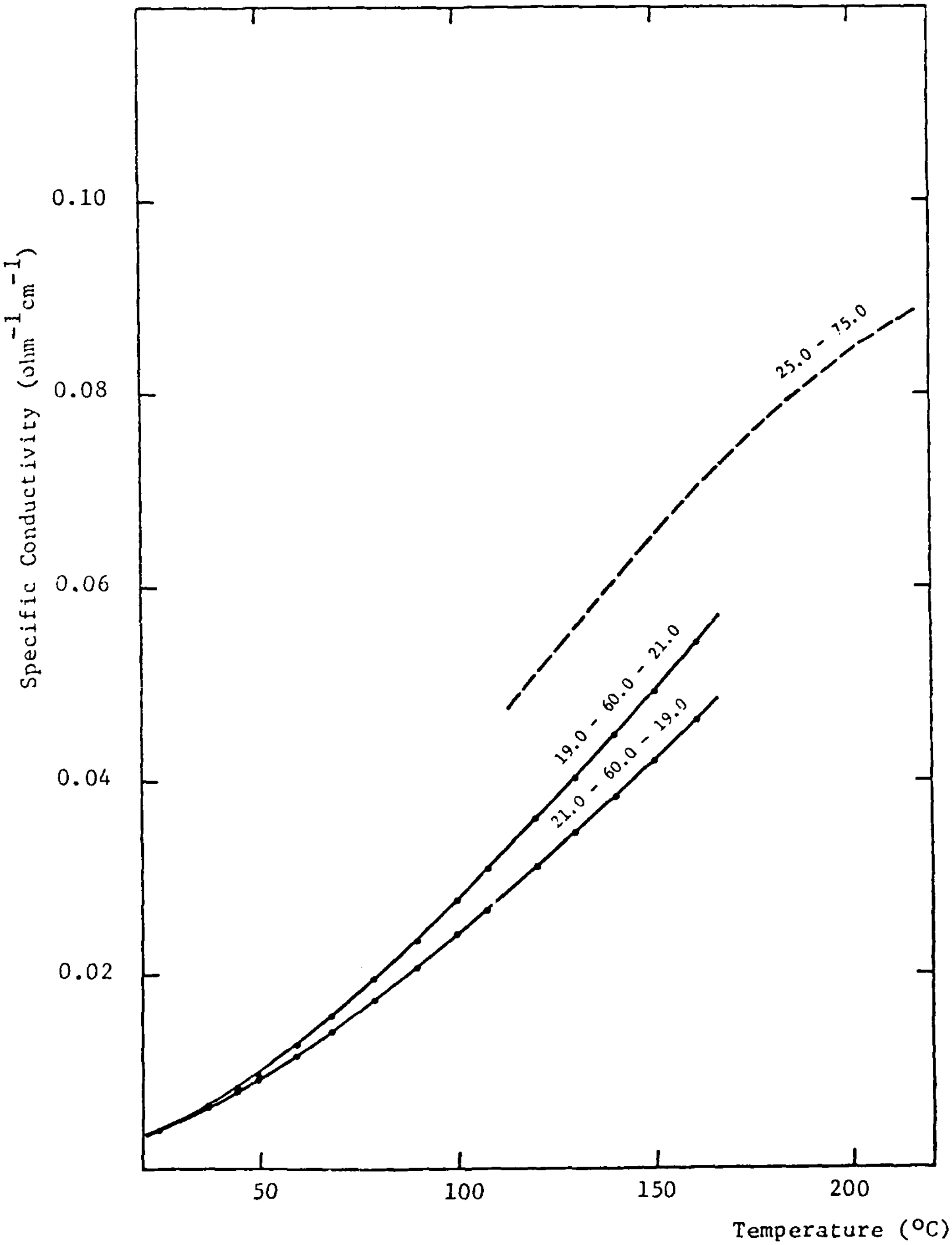

Figure 10. Specific Conductivity of $AlCl_3$-$SbCl_3$-n-BuPyCl System (Full Line) and $AlCl_3$-$SbCl_3$ (Dashed Line). Composition in mole % is indicated on the curves.

X. $FeCl_3$-NaCl SYSTEM

The phase diagram of the $FeCl_3$-NaCl system, based on the data of Morozov et al., (10), is shown in Figure 11. It is qualitatively similar to the phase diagram of the $AlCl_3$-NaCl system, shown for comparison in the same figure. In both systems a compound with 1:1 stoichiometry is formed in the solid phase, $NaFeCl_4$ and $NaAlCl_4$, respectively, and only one eutectic point exists in the acidic composition region in each case. However, the eutectic composition in the $FeCl_3$-NaCl system is close to 51 mole % $FeCl_3$, i.e., it is shifted by about 10 mole % from the eutectic composition in the $AlCl_3$-NaCl system. Also, the eutectic temperature in the $FeCl_3$-NaCl system is relatively high (156°C) compared to that of 115°C in the $AlCl_3$-NaCl system. As a result of these two differences, the liquidus temperature in the $FeCl_3$-NaCl melts is about 80°C higher than the liquidus temperature of the corresponding $AlCl_3$-NaCl melts in the 60 to 80 mole % region.

Our conductivity data for the $FeCl_3$-NaCl system are listed in Tables 31 to 34, and shown in Figure 12. The specific conductivity vs. temperature plots are linear and qualitatively similar to the conductivity plots for the $AlCl_3$-LiCl-NaCl melts. However, the specific conductivity of the $FeCl_3$-NaCl melts is higher than the specific conductivity of the corresponding $AlCl_3$-LiCl-NaCl melts, which is shown for comparison in Figure 12. Thus, the conductivity of the 52.0-48.0 mole % $FeCl_3$-NaCl melt is ∿ 10% higher than the conductivity of the 52.0-24.0-24.0 mole % $AlCl_3$-LiCl-NaCl melt at the same temperature. This difference increases to ∿ 16% for the 56.0-44.0 mole % melt, and becomes as high as ∿ 25% for the 64.0-36.0 mole % $FeCl_3$-NaCl melt when its conductivity is extrapolated to lower temperatures.

The reproducibility of our conductivity measurements on the $FeCl_3$-NaCl melts was not very good. The platinum electrodes in the conductivity cells were attacked by the melt. The cause of this problem is not clear. The $FeCl_3$ used to prepare our melts (Alfa-Ventron, anhydrous) was distilled in vacuum before use, but some residual oxychloride or $FeCl_2$ may have been still present in the purified product.

The $FeCl_3$-NaCl melts appear to be promising only for batteries in which $FeCl_3$ is used as a cathode material. The important drawback of these melts is their high liquidus temperature. It is expected, however, that this drawback can be minimized by introducing a third component, such as another alkali chloride, into the $FeCl_3$-NaCl system.

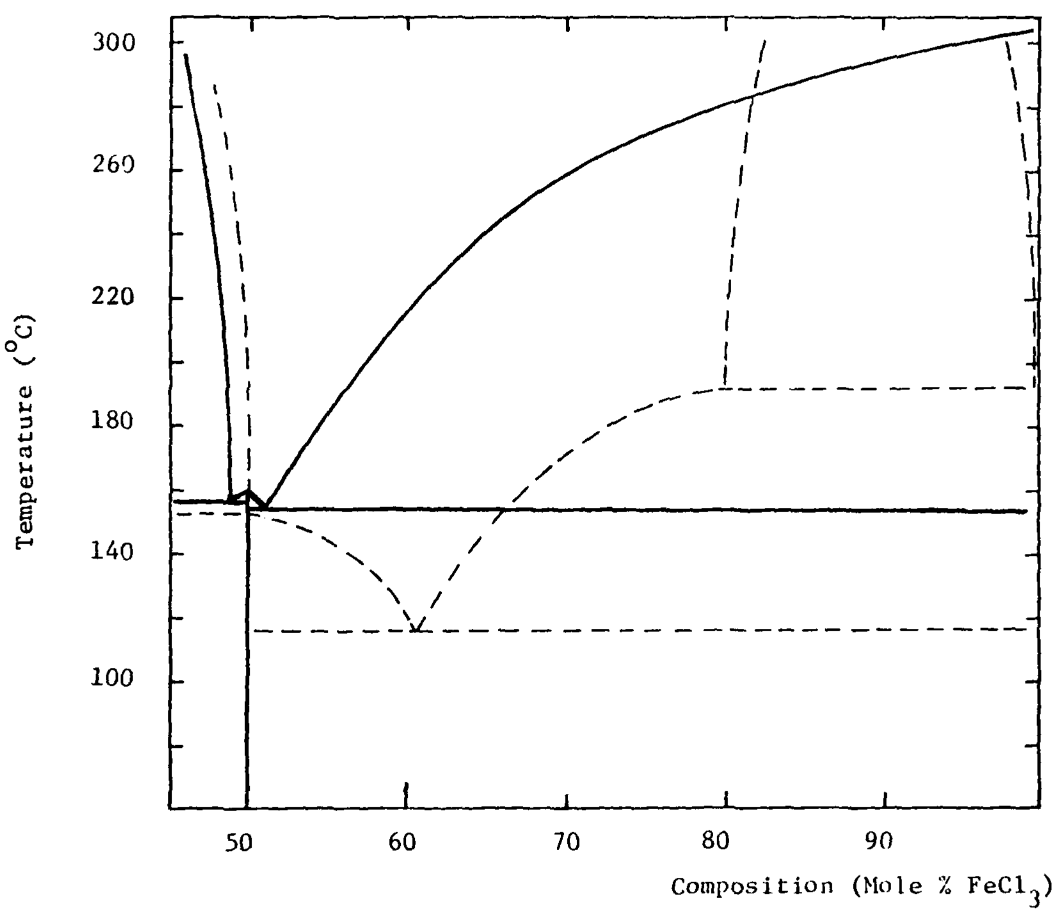

Figure 11. Phase Diagrams of the $FeCl_3$-NaCl System (Full Line) and $AlCl_3$-NaCl System (Dashed Line).

Table 31

Specific Conductivity Data for $FeCl_3$-NaCl System at 1.0 KHz

Composition: 52.0 - 48.0 (Mole %)

Temperature (°C)	Specific Conductivity ($ohm^{-1}cm^{-1}$)
182.8	0.4318
193.6	0.4611
204.2	0.4901
213.4	0.5157
223.2	0.5420
233.6	0.5682
244.0	0.5953
253.6	0.6196
263.7	0.6477
273.2	0.6686
286.0	0.6997
298.2	0.7290
310.4	0.7579
320.2	0.7794
330.1	0.7986
337.1	0.8148
348.2	0.8389

Table 32

Specific Conductivity Data for $FeCl_3$-NaCl System at 1.0 KHz

Composition: 54.0 - 46.0 (Mole %)

Temperature (°C)	Specific Conductivity ($ohm^{-1}cm^{-1}$)
236.7	0.5462
247.1	0.5715
258.3	0.5984
267.4	0.6201
277.2	0.6428
286.4	0.6635
297.7	0.6895
305.7	0.7072
315.8	0.7309
325.0	0.7524
331.7	0.7654
342.7	0.7869

Table 33

Specific Conductivity Data for $FeCl_3$-NaCl System at 1.0 KHz

Composition: 56.0 - 44.0 (Mole %)

Temperature (°C)	Specific Conductivity ($ohm^{-1}cm^{-1}$)
232.0	0.4789
249.0	0.5184
260.2	0.5428
276.4	0.5786
289.2	0.6015
302.4	0.6277
308.7	0.6406
316.2	0.6551
326.2	0.6746
333.1	0.6879
341.5	0.7070
346.8	0.7156
350.8	0.7261

Table 34

Specific Conductivity Data for $FeCl_3$-NaCl System at 1.0 KHz

Composition: 64.0 - 36.0 (Mole %)

Temperature (°C)	Specific Conductivity ($ohm^{-1} cm^{-1}$)
286.8	0.4443
297.0	0.4612
307.4	0.4779
320.2	0.4986
331.6	0.5177
341.9	0.5311
350.0	0.5436

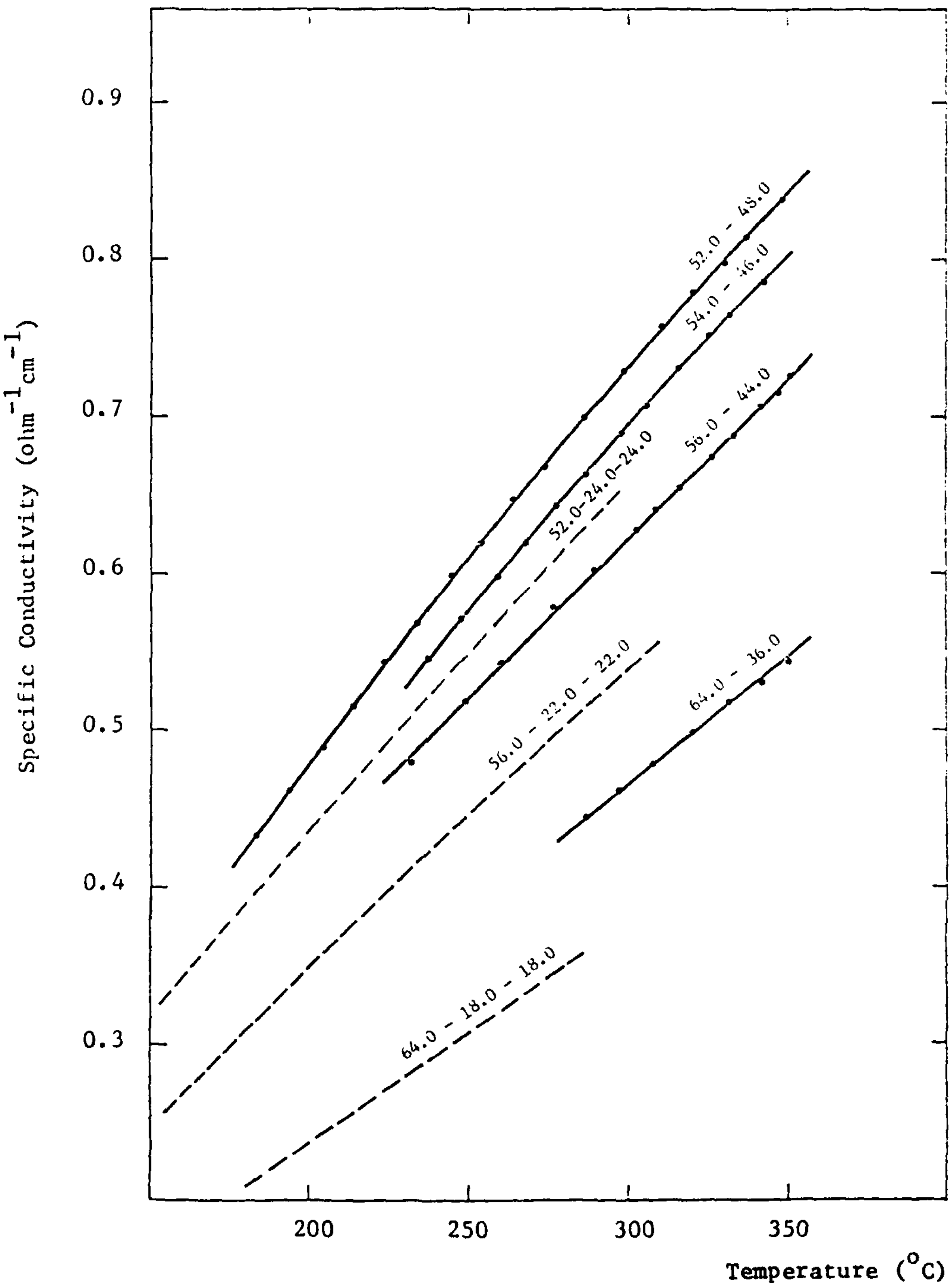

Figure 12. Specific Conductivity of $FeCl_3$-NaCl System (Full Line) and $AlCl_3$-LiCl-NaCl System (Dashed Line).
Composition in mole % is indicated on the curves.

XI. $FeCl_3$-LiCl-NaCl SYSTEM

Our specific conductivity data for the $FeCl_3$-LiCl-NaCl system are listed in Table 35 and shown in Figure 13. The specific conductivity vs. temperature plot for the 56.0-22.0-22.0 mole % melt is virtually identical to the conductivity plot for the 56.0-44.0 mole % $FeCl_3$-NaCl melt, which is also shown in the same figure. The specific conductivity of the $FeCl_3$-LiCl-NaCl melt is, therefore, ∿ 10% higher than the conductivity of the 56.0-22.0-22.0 mole % $AlCl_3$-LiCl-NaCl melt at the same temperature (Figure 13).

The problem with impurities in the ferric chloride, discussed in the previous section, was even more evident during the present measurements. Since the conductivity measurements were extended to lower temperatures than in the case of $FeCl_3$-NaCl melts, the freezing out of the impurities in the conductivity cells was considerably more pronounced. As a consequence, not only the composition of the melt was changed, but the deposition of the solid phase in the conductivity cell was effectively changing the cell constant during the measurement. Therefore, the data obtained below 220°C were not reproducible and were discarded. Conductivity measurements on the other compositions of the $FeCl_3$-LiCl-NaCl melts were postponed until ferric chloride of better purity becomes available.

Liquidus temperatures in the $FeCl_3$-LiCl-NaCl system are visually estimated to be 40 to 50°C lower than in the $FeCl_3$-NaCl system at the equivalent compositions. The literature value for the eutectic temperature of the $FeCl_3$-LiCl-KCl system is as low as 109-110°C (11, 12). The differential scanning calorimetry measurements on this system will be performed on the melts prepared with a better quality ferric chloride.

In summary, the liquidus temperatures of the $FeCl_3$-LiCl-NaCl system appear to be in approximately the same range as the liquidus temperatures of the $AlCl_3$-NaCl system. The specific conductivity of the $FeCl_3$-LiCl-NaCl system competes favorably with the conductivity of the $AlCl_3$-NaCl system. Moreover, ferric chloride is relatively inexpensive. Based on our preliminary results, therefore, the $FeCl_3$-LiCl-NaCl system is quite promising for batteries in which $FeCl_3$ is used as a cathode material. However, this system clearly requires more study.

Table 35

Specific Conductivity Data for $FeCl_3$-LiCl-NaCl System at 1.0 KHz

Composition: 56.0 - 22.0 - 22.0 (Mole %)

Temperature (°C)	Specific Conductivity ($ohm^{-1}cm^{-1}$)
226.6	0.4681
236.4	0.4911
246.2	0.5126
256.0	0.5363
265.9	0.5569
275.6	0.5754
302.8	0.6380
312.0	0.6572
322.8	0.6766

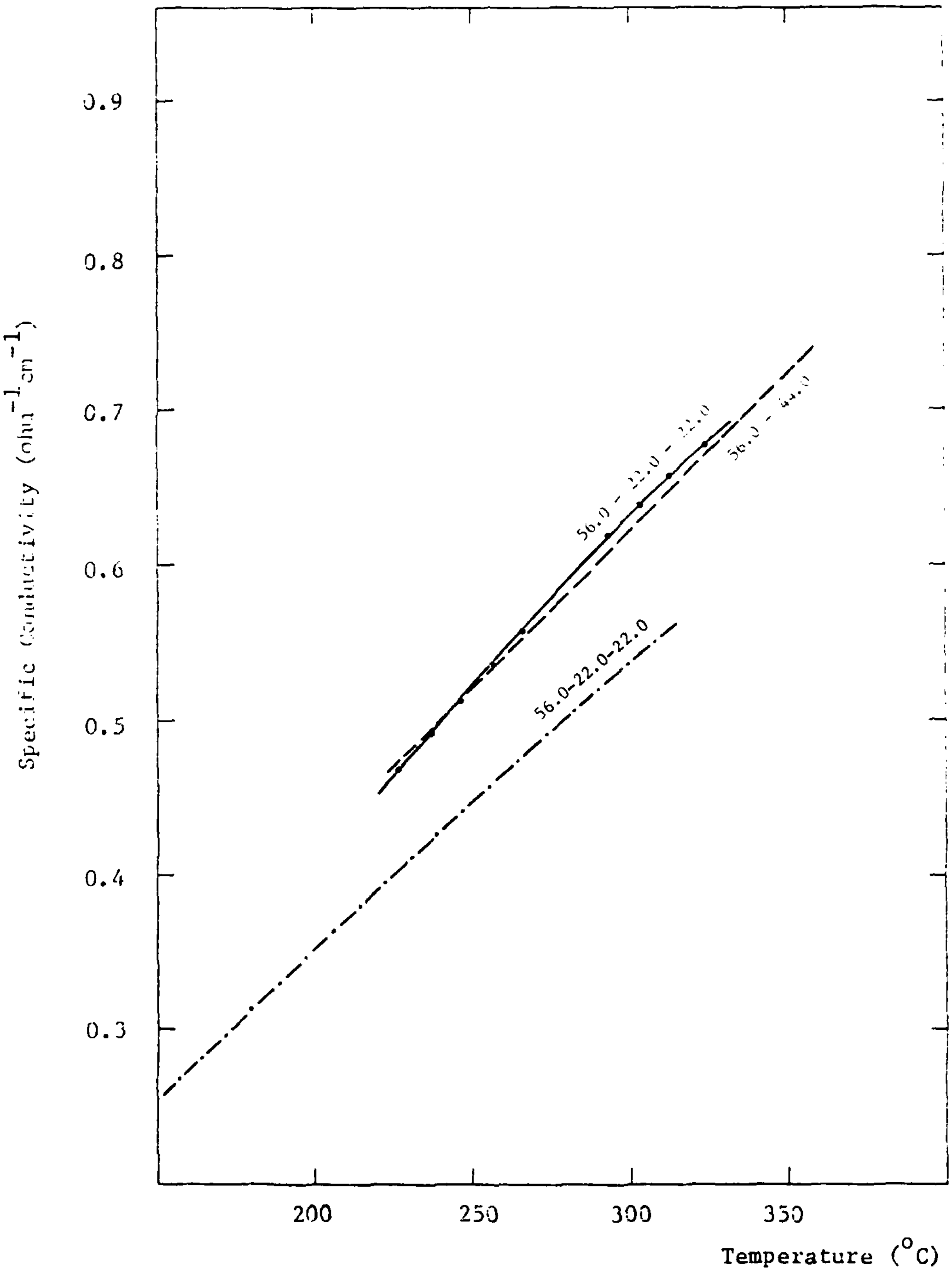

Figure 13. Specific Conductivity of $FeCl_3$-LiCl-NaCl 56.0-22.0-22.0 Mole % Melt, $FeCl_3$-NaCl 56.0-44.0 Mole % Melt (Dashed Line) and $AlCl_3$-LiCl-NaCl 56.0-22.0-22.0 Mole % Melt (Dot-dash Line). Composition in mole % is indicated on the curves.

XII. $GaCl_3$-NaCl SYSTEM

The phase diagram of the $GaCl_3$-NaCl system, based on the data of Fedorov et al, (13) is shown in Figure 14. The most conspicuous difference between this phase diagram and the phase diagram of the $AlCl_3$-NaCl system, shown in the same figure, is that the 1:1 compound, $NaGaCl_4$, melts incongruently (solidus temperature 238°C, liquidus temperature $\sim$ 450°C). The other important difference is the very low eutectic temperature of 62°C in the $GaCl_3$-NaCl system. However, due to the very low melting point of pure $GaCl_3$ compared to $NaGaCl_4$, the eutectic composition is displaced to 95 mole % $GaCl_3$. As a consequence, the liquidus temperatures in this system are higher than in the $AlCl_3$-NaCl system in the melts with less than $\sim$ 74 mole % $GaCl_3$. In the 50 to 65 mole % $GaCl_3$ region this difference is as high as 70°C or more. The low melting compositions of the $GaCl_3$-NaCl melts are between 90 and 100 mole % $GaCl_3$, i.e., in the region where the volatility, as well as the acidity of the melts, is quite high.

Our specific conductivity data for the $GaCl_3$-NaCl system are listed in Tables 36 to 38 and shown in Figure 15. The conductivity vs. temperature plots are linear. The specific conductivity of the 70.0-30.0 mole % $GaCl_3$-NaCl melt is 15 to 20% higher than the conductivity of the 68.0-24.0-8.0 mole % $AlCl_3$-LiCl-NaCl melt, which has a comparable content of the acidic component. The conductivities for the $GaCl_3$-KCl, $GaCl_3$-RbCl and $GaCl_3$-CsCl systems, which are available in literature (14), are slightly lower. The substantial decrease of the conductivity in the melts with 80.0 and 90.0 mole % $GaCl_3$ reflects a drop in the concentration of Na^+ ions, which are presumably charge carriers in these melts.

Only high purity $GaCl_3$ is commercially readily available at present and its cost is high. Perhaps the more important drawback, however, is the fact that the low melting (< 100°C) region of $GaCl_3$-NaCl melts is the narrow region above $\sim$ 90 mole % $GaCl_3$. This is the region of low specific conductivity as well as of high volatility, both undesirable melt properties from the battery use standpoint.

XIII. CONCLUSIONS

On the basis of the phase diagram and specific conductivity data presented in this Report, four molten salt systems emerge as the most promising for battery applications: $AlCl_3$-LiCl-NaCl, $AlCl_3$-$SbCl_3$-MCl

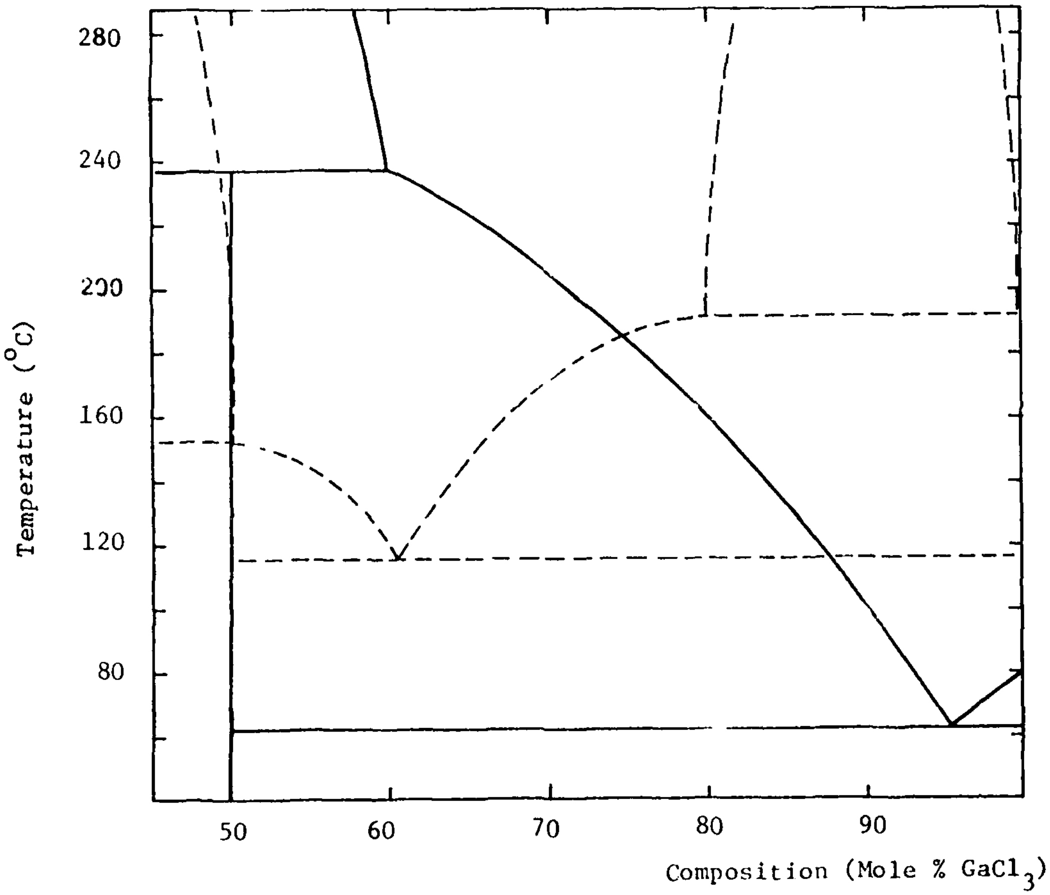

Figure 14. Phase Diagrams of the $GaCl_3$-NaCl System (Full Line) and $AlCl_3$-NaCl System (Dashed Line).

Table 36

Specific Conductivity Data for $GaCl_3$-NaCl System at 1.0 KHz

Composition: 70.0 - 30.0 (Mole %)

Temperature (°C)	Specific Conductivity ($ohm^{-1}cm^{-1}$)
158.1	0.1626
165.3	0.1730
172.0	0.1824
179.5	0.1933
186.1	0.2029
193.7	0.2134
200.5	0.2239
211.5	0.2397
219.2	0.2514
227.6	0.2647
237.0	0.2790

Table 37

Specific Conductivity Data for $GaCl_3$-NaCl System at 1.0 KHz

Composition: 79.6 - 20.4 (Mole %)

Temperature (°C)	Specific Conductivity ($ohm^{-1}cm^{-1}$)
145.9	0.0946
153.0	0.1009
160.6	0.1075
166.8	0.1130
175.4	0.1206
182.2	0.1265
189.9	0.1332
201.4	0.1428
209.0	0.1503
217.5	0.1584
225.7	0.1668

Table 38

Specific Conductivity Data for $GaCl_3$-NaCl System at 1.0 KHz

Composition: 90.0-10.0 (Mole %)

Temperature (°C)	Specific Conductivity ($ohm^{-1}cm^{-1}$)
110.8	0.02618
118.6	0.02859
125.3	0.03075
132.2	0.03292
138.7	0.03498
145.4	0.03706
151.5	0.03902
163.7	0.04174
170.1	0.04368
175.0	0.04533
182.3	0.04789
190.4	0.05063
197.7	0.05326
206.1	0.05689
211.1	0.05886
220.9	0.06328

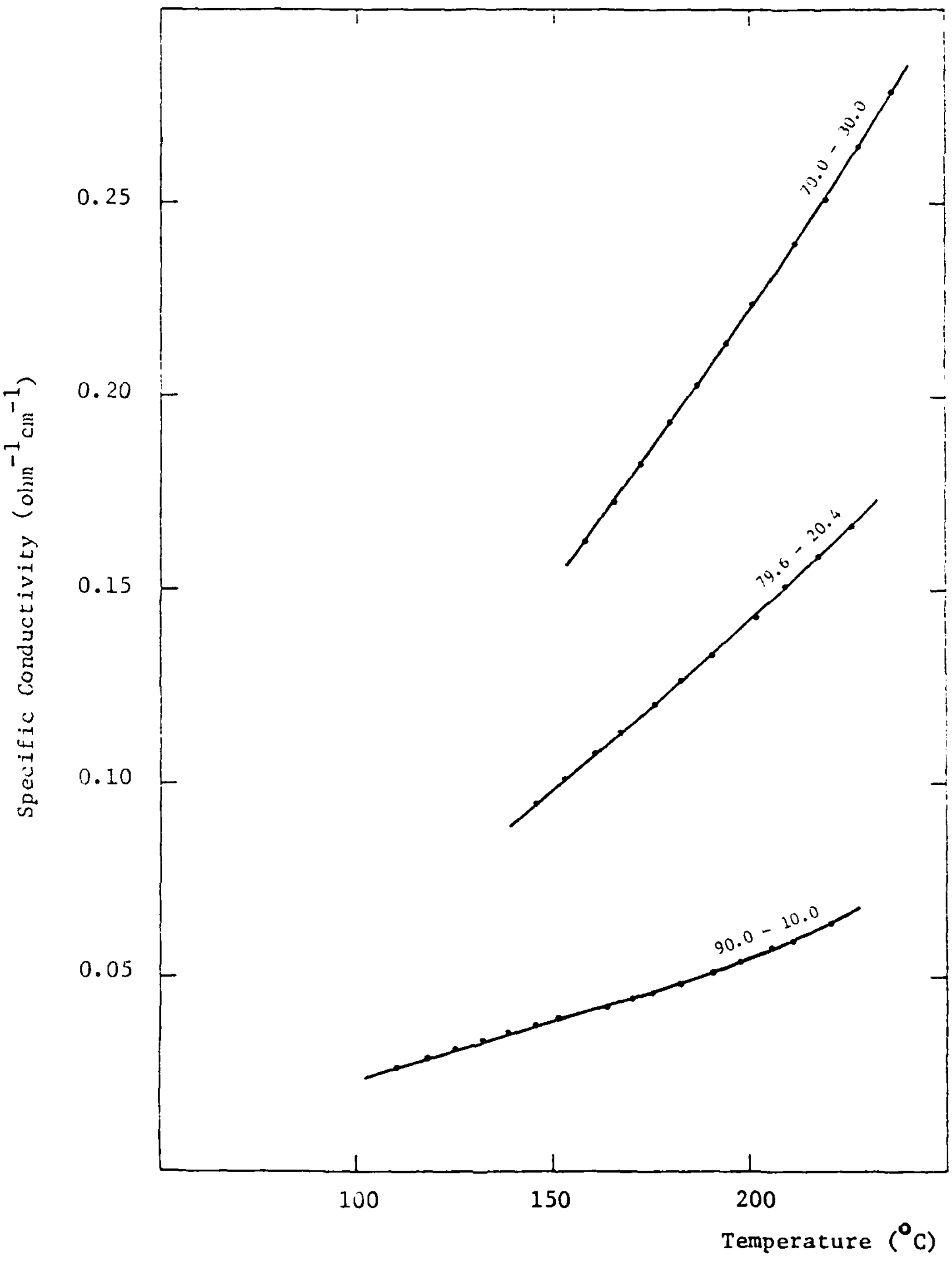

Figure 15. Specific Conductivity of $GaCl_3$-NaCl System. Composition in mole % is indicated on the curves.

(where MCl stands for an alkali chloride), $FeCl_3$-LiCl-NaCl and, possibly, $AlCl_3$-Bu_4NCl.

The addition of LiCl to the binary $AlCl_3$-NaCl melts, the most widely used of the chloroaluminate melts, significantly lowers the liquidus temperature of these melts. The specific conductivity of the $AlCl_3$-LiCl-NaCl melts is not substantially lower than the conductivity of the $AlCl_3$-NaCl melts. Therefore, the $AlCl_3$-LiCl-NaCl system remains one of the most promising low melting molten salt systems for further study.

The $AlCl_3$-$SbCl_3$ system is promising for use in batteries which employ $SbCl_3$ as a cathode material. The liquidus temperatures in this system are low, and, considering the molecular character of the melt constituents, $AlCl_3$ and $SbCl_3$, the specific conductivity of the $AlCl_3$-$SbCl_3$ melts is relatively high. Compared to the conductivity of the $AlCl_3$-LiCl-NaCl melts in the same temperature range, however, the conductivity of the $AlCl_3$-$SbCl_3$ melts is lower by a factor of five. Therefore, it is desirable to attempt to improve the specific conductivity of the $AlCl_3$-$SbCl_3$ melts by adding another ionic component to these melts. The most promising $SbCl_3$-containing molten salt system for further study is probably $AlCl_3$-$SbCl_3$-MCl, where MCl is an alkali chloride.

The specific conductivity of the two $FeCl_3$-based molten salt systems is higher than the conductivity of the $AlCl_3$-LiCl-NaCl system. The liquidus temperatures in the $FeCl_3$-LiCl-NaCl system, the lower melting of the two $FeCl_3$-containing systems, appear to be in the same range as the liquidus temperatures in the $AlCl_3$-NaCl melts. The $FeCl_3$-LiCl-NaCl system, therefore, is quite promising for batteries which employ $FeCl_3$ as a cathode material.

No data are presented in this report for the $AlCl_3$-Bu_4NCl system. In view of the low melting point of the pure Bu_4NCl salt and its strongly ionic character, as well as our experience with the $AlBr_3$-R_4NBr systems, the $AlCl_3$-Bu_4NCl system is probably the most promising system of the $AlCl_3$-R_4NCl type.

Further work on the present project will concentrate on the four molten salt systems singled out in this section.

REFERENCES

1. Technical Report AFAPL-TR-79-2124, November 1979.
2. R. A. Carpio, F. C. Kibler, Jr., L. A. King, W. Brokner, K. Tørklep and H. A. Øye, Ber. Bunsenges. Phys. Chem. (in press).
3. E. Ya. Gorenbein, Zhur. Obshch. Khim., 18, 1427 (1948); 19, 1978 (1949).
4. J. A. Plambeck, J. Chem. Eng. Data, 12, 77 (1967).
5. J. C. Goodrich, F. M. Goyan, E. E. Morse, R. G. Preston and M. B. Young, J. Am. Chem. Soc., 72, 4411 (1950); T. R. Griffiths, J. Chem. Eng. Data, 8, 568 (1963); M. B. Reynolds and C. A. Kraus, J. Am. Chem. Soc., 70, 1709 (1948).
6. Handbook of Chemistry and Physics, 57th edition, Cleveland, 1977, p. C-105.
7. J. Kendall, E. D. Crittenden and H. K. Miller, J. Am. Chem. Soc., 45, 976 (1923).
8. L. A. Nisel'son, Z. N. Orshanskaya, and K. V. Tret'yakova, Zh. Neorg. Khim., 19, 1060 (1974).
9. R. Huglen, G. Mamantov, G. M. Begun and G. P. Smith, J. Raman Spectr., 9, 188 (1980).
10. I. S. Morozov and D. Ya. Toptygin, Zhur. Neorg. Khim., 2, 2133 (1957).
11. A. V. Storonkin, I. V. Vasil'kova, and M. D. Pyatunin, Russ. J. Phys. Chem., 47, 25 (1973).
12. M. D. Pyatunin, A. V. Storonkin, and I. V. Vasil'kova, Vestnik Leningrad Univ., Ser. Fiz Khim., 165 (1973).
13. P. I. Fedorov and V. M. Yakunina, Russ. J. Inorg. Chem., 8, 1099 (1963).
14. V. N. Arbekov and E. S. Petrov, Izv. Sibirsk. Otd. ANSSSR, Ser. Khim. Nauk, 133 (1968).